Molecular Vibrations of Zirconium(IV) Tetrahydroborate, a Compound containing Triple Hydrogen Bridges

By **Brian E. Smith, Herbert F. Shurvell, and Bruce D. James,*†** University of Queensland, St. Lucia Queensland, Australia

The i.r. and Raman spectra of Nujol solutions and solid samples of both $Zr(BH_4)_4$ and $Zr(BD_4)_4$ are reported. The assignments of the observed spectra are discussed on the basis of both T and T_d symmetry point groups. Significant contributions to the $Zr(BD_4)_4$ spectra of ^1H-containing species are observed. A modified valence force field incorporating an explicit Zr–B stretching force constant (1.5 mdyn $Å^{-1}$) is developed. Qualitative descriptions of the normal vibrations are made on the basis of calculated potential-energy distributions.

ZIRCONIUM(IV) TETRAHYDROBORATE, $Zr(BH_4)_4$, was the first molecule recognized to contain a trihydrogen-bridged MH_3BH_t group.‡ It was concluded, from an X-ray diffraction study of crystalline $Zr(BH_4)_4$,[1] that there was a tetrahedral $Zr(BH_t)_4$ 'skeleton' with triple hydrogen bridges between the metal and each boron atom, and that in the absence of disorder the molecule would conform to full T_d symmetry. Subsequent studies by vibrational spectroscopy[2,3] confirmed the presence of both triple hydrogen bridging and a high molecular symmetry.

The reported space group[1] was T_d^1 ($P\bar{4}3m$), with one

† *Present address:* Department of Inorganic and Analytical Chemistry, La Trobe University, Bundoora, Victoria 3083, Australia.

‡ The subscript, t, is used to distinguish the terminal from the bridging hydrogen atoms.

[1] P. H. Bird and M. R. Churchill, *Chem. Comm.*, 1967, 403.
[2] T. J. Marks, W. J. Kenelly, J. R. Kolb, and L. A. Shimp, *Inorg. Chem.*, 1973, **11**, 2540.
[3] N. Davies, M. G. H. Wallbridge, B. E. Smith, and B. D. James, *J.C.S. Dalton*, 1973, 162.

molecule per unit cell. This requires that the site symmetry be T_d. However, it was pointed out that the bridging hydrogen atoms were not located reliably so that T_d molecular symmetry for $Zr(BH_4)_4$ was not definitely established. A more recent electron-diffraction study of the vapour [4] indicated that the orientations of the BH_4 groups about the Zr–B bond vectors were such that the bridging hydrogen atoms were staggered with respect to the three distant Zr–B bonds. Therefore, $Zr(BH_4)_4$ has T molecular symmetry in the vapour phase. Further refinement of the electron-diffraction intensities led to an estimate of the torsional angle $\phi = 38°$ ($\phi = 0$ corresponds to the eclipsed conformation of the hydrogen bridges and Zr–B bonds). Diagrams of the eclipsed and two staggered structures are given in ref. 5. Over the past decade a number of other tetrahydroborates also have been suggested, mainly on the basis of data from vibrational spectroscopy and diffraction methods, to incorporate a triply bridged structure.[2-19]

Despite the formidable size of $Zr(BH_4)_4$, in vibrational spectroscopic terms, it seemed to us that the high symmetry of this system might allow an analysis sufficient to characterize the vibrations of a ZrH_3BH_t group in some detail. Improved facilities over those of ref. 3 have resulted in a useful extension of vibrational data and more complete assignments of the spectra are now possible. The structural implications of the current data have been considered separately.[5] It was concluded that the observations are more readily interpreted on the assumption of a T rather than a T_d molecular symmetry for $Zr(BH_4)_4$ in agreement with the electron-diffraction results. In this paper we present details of i.r. and Raman spectra of solution and solid phases of $Zr(BH_4)_4$ and $Zr(BD_4)_4$. An attempt is made to give a complete assignment of the fundamentals of both molecules, together with qualitative descriptions of the modes based on potential-energy distributions obtained from a normal co-ordinate analysis.

EXPERIMENTAL

Zirconium(IV) tetrahydroborate and the corresponding tetradeuterioborate $Zr(BD_4)_4$ were prepared and purified as described previously.[18] Infrared spectra were recorded using a Perkin-Elmer 225 spectrometer.

Liquid paraffin (Nujol) solvent was dried by refluxing over CaH_2 under a nitrogen atmosphere. It was then filtered through diatomaceous earth (pre-dried by extended evacuation on a vacuum line) in a nitrogen-filled glove-box. Solutions were made up on a vacuum line, taking precautions to minimize impurities. For solution i.r. measurements either (*a*) a conventional solution cell (KBr plates, 0.1-mm spacer) fitted with Teflon stoppers, or (*b*) a more concentrated sample pressed between KBr or CsI plates was used. The latter procedure yielded less interference from solvent peaks and, apart from some initial decomposition from material exuded at the periphery, the sample was long-lived. Spectra from both sampling techniques were identical.

The liquid-nitrogen cryostat for solid-phase i.r. measurements was made in the workshops of the University of Queensland. The sample was deposited rapidly on to a CsI plate in thermal contact with a cold finger containing liquid nitrogen. The external windows were also of CsI so that spectra could be recorded down to 200 cm^{-1}. Although the temperature of the deposition-plate holder was maintained at 77 K, the actual temperature of the sample may have been higher due to local heating by the i.r. radiation. In each of the many i.r. spectra recorded, cell blanks were run both before and after sample deposition. In no case were residual impurities detected.

Raman spectra were recorded using a Cary 82 spectrometer and were excited by the 514.5- and 488.0-nm lines from an argon-ion laser. Laser and plasma lines were used to calibrate the instrument and the wavenumbers reported in the Tables are believed to be accurate to within ± 1.0 cm^{-1}. Raman spectra of Nujol solutions of $Zr(BH_4)_4$ and $Zr(BD_4)_4$ were recorded at room temperature and spectra of polycrystalline films were obtained at liquid-nitrogen temperature.

Samples were deposited on a copper block cooled in a liquid-transfer cryostat (Oxford Instruments Ltd.). The gas to be deposited, after passing through a needle valve, was sprayed directly on to the copper block. Temperatures were measured by means of a carbon resistance thermometer mounted above the sample block. The temperature was maintained at 77 K throughout the experiments. However, the actual temperature of the sample may have been higher due to local heating by the laser beam.

All the i.r. and Raman spectra of the two compounds in the solid phase and in solution displayed a high degree of consistency. The only variations observed pertain to solid-phase Raman spectra of $Zr(BH_4)_4$, where some showed poorer resolution than others. It seems unlikely that any but the weakest of the features reported are derived from impurities.

RESULTS AND DISCUSSION

The following spectra of $Zr(BH_4)_4$ and $Zr(BD_4)_4$, respectively, are shown: i.r. Nujol solution (Figures 1

[4] V. Plato and K. Hedberg, *Inorg. Chem.*, 1971, **10**, 590.
[5] B. D. James, B. E. Smith, and H. F. Shurvell, *J. Mol. Structure*, 1976, **33**, 91.
[6] B. D. James, B. E. Smith, and M. G. H. Wallbridge, *J. Mol. Structure*, 1972, **14**, 327.
[7] E. R. Bernstein, W. C. Hamilton, T. A. Keiderling, S. J. La Placa, S. J. Lippard, and J. J. Mayerle, *Inorg. Chem.*, 1972, **11**, 3009.
[8] T. A. Keiderling, W. T. Wozniak, R. S. Gray, D. Jurkowitz, E. R. Bernstein, S. J. Lippard, and T. G. Spiro, *Inorg. Chem.*, 1975, **14**, 576.
[9] M. Ehemann and H. Nöth, *Z. anorg. Chem.*, 1971, **386**, 87.
[10] V. V. Volkov, K. G. Myakishev, and Z. A. Grankina, *Russ. J. Inorg. Chem.*, 1970, **15**, 1490.
[11] K. Franz and H. Nöth, *Z. anorg. Chem.*, 1973, **397**, 247.
[12] J. W. Nibler, *J. Amer. Chem. Soc.*, 1972, **94**, 3349.
[13] D. S. Marynick and W. N. Lipscomb, *J. Amer. Chem. Soc.*, 1973, **95**, 7244.
[14] G. Gundersen, L. Hedberg, and K. Hedberg, *J. Chem. Phys.*, 1973, **59**, 3777.
[15] K. Brendhaugen, A. Haaland, and D. P. Novak, *Acta Chem. Scand.*, 1975, **A29**, 801.
[16] T. J. Marks and J. R. Kolb, *J. Amer. Chem. Soc.*, 1975, **97**, 27.
[17] T. J. Marks and G. W. Grynkewich, *Inorg. Chem.*, 1976, **15**, 1302.
[18] B. D. James and B. E. Smith, *Synth. React. Inorg. Metal-Org. Chem.*, 1974, **4**, 461.
[19] J. Tomkinson and T. C. Waddington, *J.C.S. Faraday II*, 1976, 1245.

TABLE 1

Observed wavenumbers (cm^{-1}) in the spectra of zirconium(IV) tetrahydroborate [a]

Solid (77 K)		Solution				
I.r.	Raman	I.r.	Raman [b]			Assignment and description
2 580 (sh)	2 578 (sh)					
2 569m	2 571m	2 567s		ν_{11}	$F(F_2)$	BH_t str.
2 563m	2 561 (sh)					
	2 580m					
	2 573s		2 566s,p	ν_1	$A(A_1)$	BH_t str.
	2 567s					
	2 210 (sh)		2 207 (sh)	ν_6	$E(E)$	BH_b str.
2 199 (sh)				ν_{12}?	$F(F_1)$	BH_b str.
2 171m	2 178 (sh)	2 180s		ν_{13}	$F(F_2)$	BH_b str.
	2 165m		2 176s,p	ν_2	$A(A_1)$	BH_b str.
	2 139 (sh)		2 100—2 145 (sh)	ν_{12}?	$F(F_1)$	alternative
2 107m	2 100 (sh)	2 115s		ν_{14}	$F(F_2)$	BH_b str.
2 186mw	1 290 (sh)	1 286w		ν_{15}	$F(F_2)$	HBH bend
	1 285s		1 283s,p	ν_3	$A(A_1)$	HBH bend
	1 283 (sh)			ν_7	$E(E)$	HBH bend
1 217s	1 215vw	1 213s		ν_{16}	$F(F_2)$	HBH bend
1 178mw		1 170 (sh)		ν_{17}	$F(F_2)$	HBH bend
1 185 (sh)	1 108w	1 098w		ν_{18}?	$F(F_1)$	HBH bend
	1 075w		1 075w,dp	ν_8	$E(E)$	HBH bend
1 058mw		1 056w		ν_{19}	$F(F_2)$	HBH bend
	610w			ν_{20}?	$F(F_2)$	Zr–BH_4 torsion
581w	581w	575 (sh)	576 (sh)	ν_{21}	$F(F_2)$	ZrH_b str. (bridge def.)
	557 (sh)					
	554s		544s,p	ν_4	$A(A_1)$	Zr–BH_4 str.
	549s					
547w	543m			ν_{22}?	$F(F_1)$	ZrH_b stretch
	533w			ν_9	$E(E)$	(bridge def.)
504s	504w	504s	505 (sh)	ν_{23}	$F(F_2)$	Zr–BH_4 str.
	ca. 275vw			ν_5?	$A(A_2)$	Zr–BH_4 torsion
	224vs		213s,dp	ν_{10}	$E(E)$	BH_4–Zr–BH_4 bend
216mw	216w (sh)	213w		ν_{24}	$F(F_2)$	
	ca. 55vvw			ν_L	$F(F_1)$	lattice mode?

[a] Relative intensities in this and subsequent Tables are indicated by s = strong, m = medium, w = weak, v = very, and sh = shoulder. [b] p = polarized, dp = depolarized.

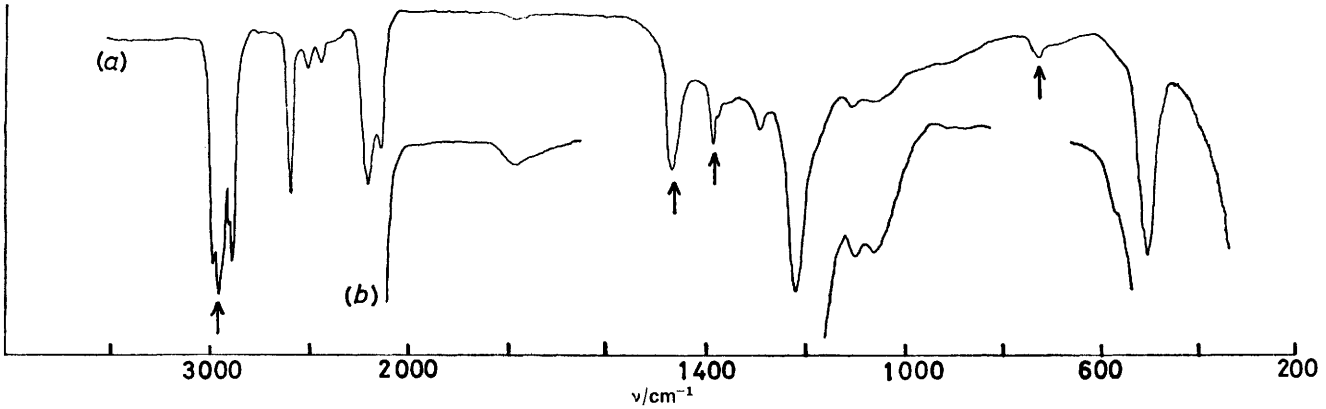

FIGURE 1 Infrared spectrum of a Nujol solution of $Zr(BH_4)_4$. Solvent peaks are marked by arrows. Spectrum (*b*) was recorded using a longer sample path length than for (*a*)

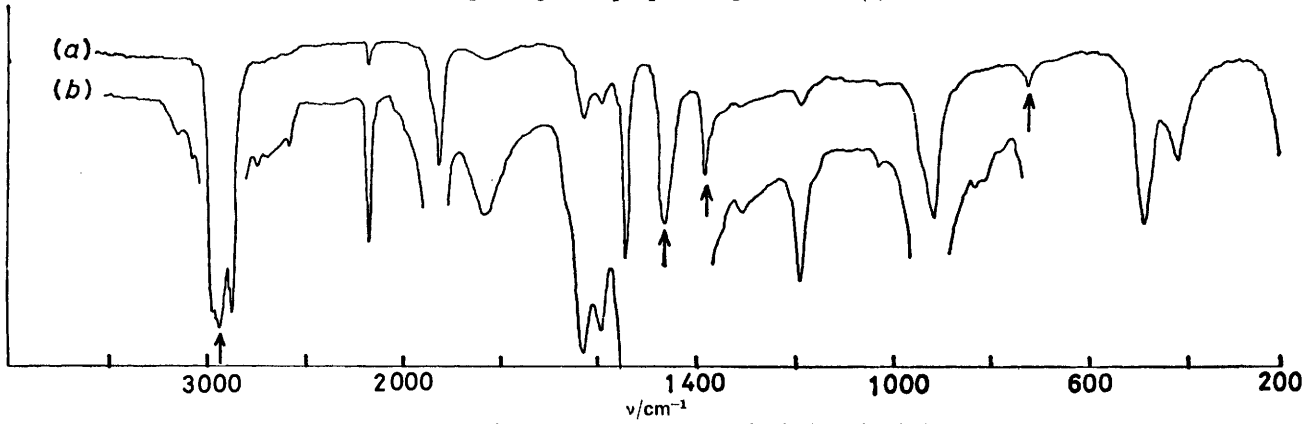

FIGURE 2 Infrared spectrum of a Nujol solution of $Zr(BD_4)_4$

and 2); Raman, Nujol solution (Figures 3 and 4); i.r., solid phase, liquid-nitrogen temperature (Figures 5 and 6); Raman, solid phase, liquid-nitrogen temperature (Figures 7 and 8). Observed frequencies, relating to all the samples, are given in Tables 1 [$Zr(BH_4)_4$], 2 [$Zr(BD_4)_4$], and 3 (overtones and combinations).

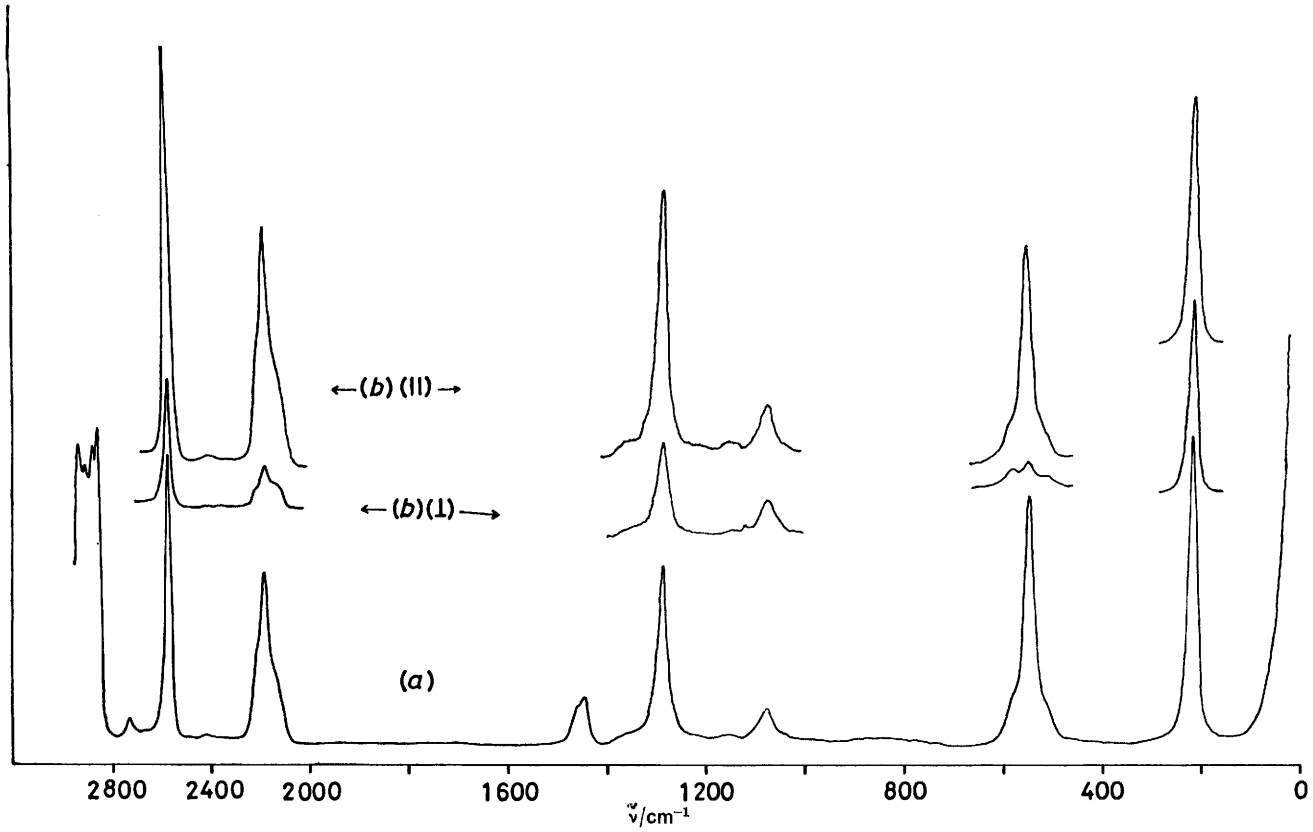

FIGURE 3 Raman spectrum of $Zr(BH_4)_4$ in Nujol solution. Spectra (*b*) were obtained with a polarizing plate between the sample and the spectrometer collecting lens

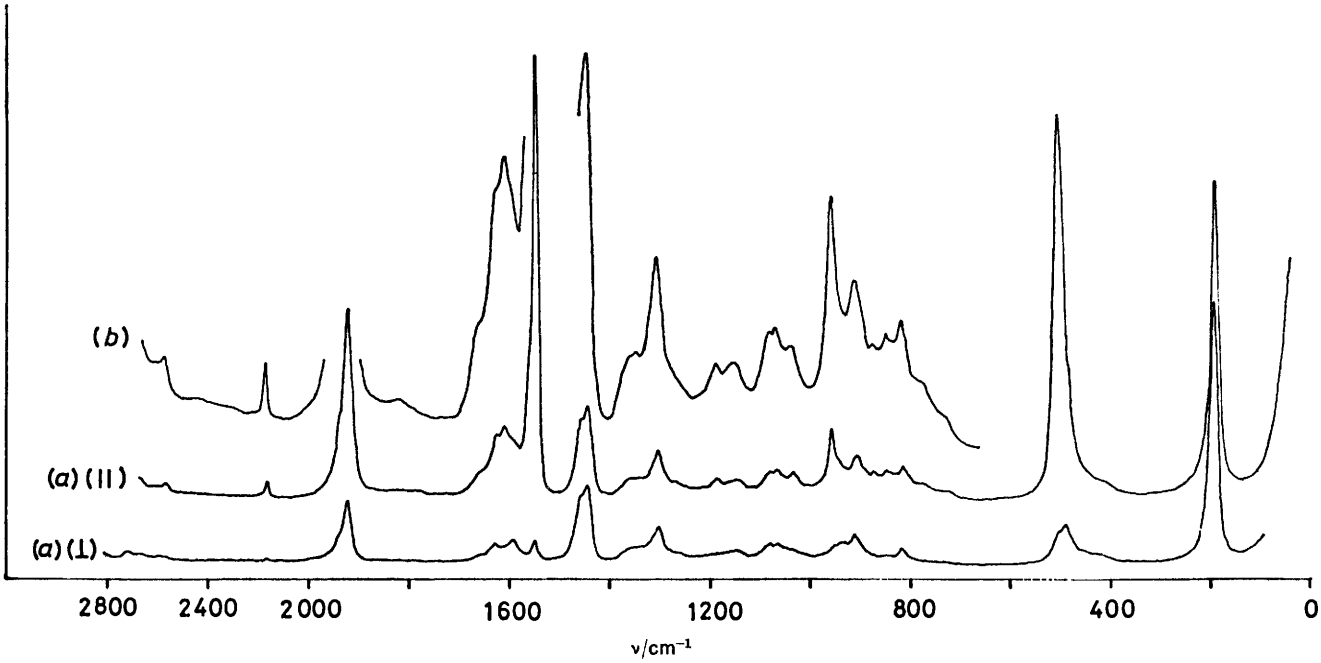

FIGURE 4 Raman spectrum of $Zr(BD_4)_4$ in Nujol solution. Spectra (*a*) were obtained with a polarizing plate between the sample and the spectrometer collecting lens; (*b*) is a vertical intensification of (*a*) (||)

Assignment of the Vibrational Spectra.—The correlation between the vibrations of a ZrH_3BH_t group of symmetry C_{3v} and those of $Zr(BH_4)_4$ molecules conforming to T_d and T symmetries is given in Table 4. The frequency regions in which the different types of vibrations are observed have largely been elucidated elsewhere.[3,5] These data are incorporated in Table 4, which forms a basis from which detailed assignments can

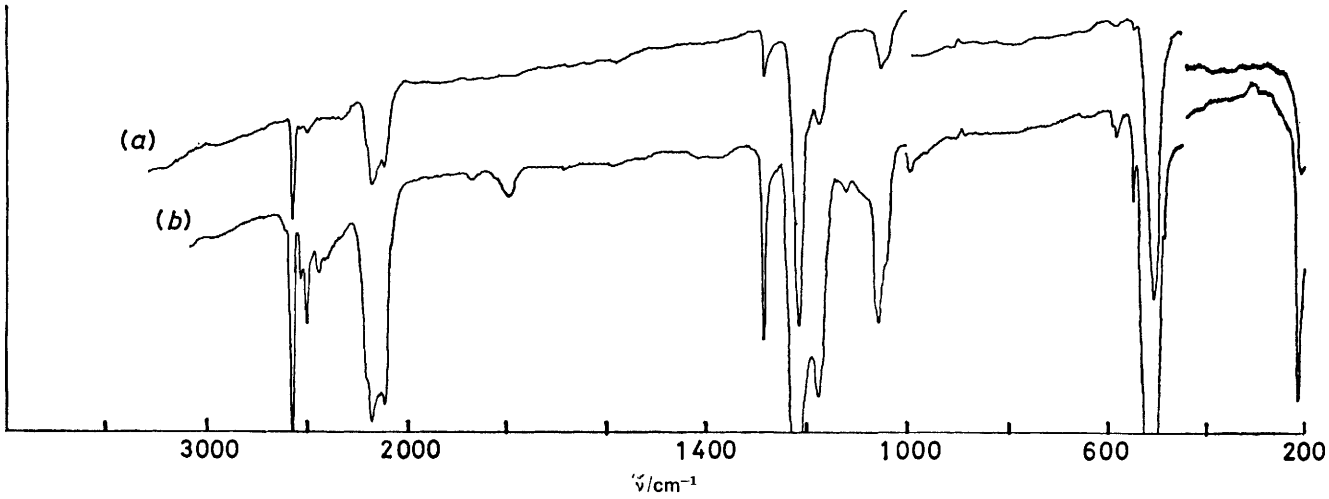

FIGURE 5 Infrared spectrum of solid $Zr(BH_4)_4$ using a liquid-nitrogen cryostat and CsI windows. Spectrum (*b*) is derived from a thicker sample deposit than (*a*)

TABLE 2

Observed wavenumbers (cm^{-1}) in the spectra of zirconium(IV) tetradeuterioborate

Solid (77 K)		Solution			
I.r.	Raman	I.r.	Raman	Assignment and description	
2 567vw	2 567vw	2 567vw	2 567vvw	^{1}H species	BH_t str.
2 164 (sh)	2 164 (sh)	2 161w	2 162vw,p	^{1}H species	BH_b str.
2 158w	2 157vw				
	1 938mw	1 935 (sh)	1 934 (sh)	^{1}H species	BD_t str.
1 924m		1 920s		ν_{11} $F(F_2)$	BD_t str.
1 920m					
	1 922s		1 919m,p	ν_1 $A(A_1)$	BD_t str.
1 658 (sh)	1 656 (sh)	1 660 (sh)	1 657 (sh)	^{1}H species	BD_b str.
1 628 (sh)	1 627 (sh)				
1 616w	1 615 (sh)	1 626mw	1 625vw	ν_{12}? $F(F_1)$	BD_b str.
1 599 (sh)	1 593w		1 606w,p	^{1}H species	BD_b str.
1 590 (sh)					
1 585w	1 585 (sh)	1 589w	1 591vw	ν_{13} $F(F_2)$	BD_b str.
1 560vw	1 559vw	1 555 (sh)	1 555—1 570 (sh)	^{1}H species	BD_b str.
1 553vw	1 553vw				
	1 544s		1 547s,p	ν_2 $A(A_1)$	BD_b str.
		1 546 (sh)		^{1}H species	BD_b str.
1 536s		1 539s		ν_{14} $F(F_2)$	BD_b str.
1 188w	1 188vw	1 185w	1 186vw,p	^{1}H species	HBD bend
	1 027vw	1 026vw			
	954w		945w,p	ν_3 $A(A_1)$	DBD bend
924m		937 (sh)		ν_{15} $F(F_2)$	DBD bend
909m		911s		ν_{16} $F(F_2)$	DBD bend
	908w		907w,dp	ν_7 $E(E)$	DBD bend
877vw				^{1}H species	HBD bend
837vw	835vw	830vw		ν_{17} $F(F_2)$	DBD bend
	817w		814vw,dp	ν_8 $E(E)$	DBD bend
811w		809vw		ν_{18}? $F(F_1)$	DBD bend
793w	793vw			ν_{19} $F(F_2)$	DBD bend
	518 (sh)				
	512s		504s,p	ν_4 $A(A_1)$	Zr–BD_4 str.
	502m				
506 (sh)		511 (sh)		^{1}H species	skeletal str.
483s	481w	484s	487w	ν_{23} $F(F_2)$	Zr–BD_4 str.
			458w	ν_{20}? $F(F_1)$	Zr–BD_4 torsion
	435vw (sh)			ν_9 $E(E)$	Zr–D_b str.
425m		418m	416 (sh)	ν_{21} $F(F_2)$	(bridge def.)
	201 (sh)			ν_5? $A(A_2)$	Zr–BD_4 torsion
	198vs		190s,dp	ν_{10} $E(E)$	BD_4–Zr–BD_4 bend
	45vw			ν_L $F(F_1)$	lattice mode?

be sought. It is noted, however, that the spectra of both the zirconium compounds consist of a superimposition of bands due to a variety of isotopic species.

Isotopic species. Assuming a random distribution of ^{10}B and ^{11}B isotopes (natural abundances 19.6 and 80.4%, respectively), the isotopic species $Zr^{10}B_n{}^{11}B_{4-n}$ occur in 41.8, 40.8, 14.9, 2.4, and 0.1% abundance for $n = 0$—4, respectively. Substitution of the lighter ^{10}B isotope for ^{11}B results in increases in the observed vibrational frequencies, distributed among the $3N - 6$ normal modes. However, since the ^{10}B–^{11}B interchange produces only a small change in reduced mass, the observed frequency effects are small and are only detected under high resolution in sharp spectral features. Thus, for example, in the low-temperature solid-phase data for $Zr(BH_4)_4$ splittings observed in the i.r.-active $B–H_t$ stretch (2 563, 2 569, and 2 580 cm^{-1}), the corresponding totally symmetric Raman mode (2 567, 2 573, and 2 580 cm^{-1}), and the skeletal $Zr–BH_4$ stretch (543, 549, 554, and 557 cm^{-1}) are ascribed to the resolution of $Zr^{10}B_n{}^{11}B_{4-n}$ frequencies.

The spectra of $Zr(BD_4)_4$ show an increased complexity due to the presence of a small overall proportion of ^1H nuclei, deriving from the $Li[BD_4]$ starting material (claimed to contain * no more than 2% ^1H). However, the presence of 1—2% of ^1H nuclei implies that between

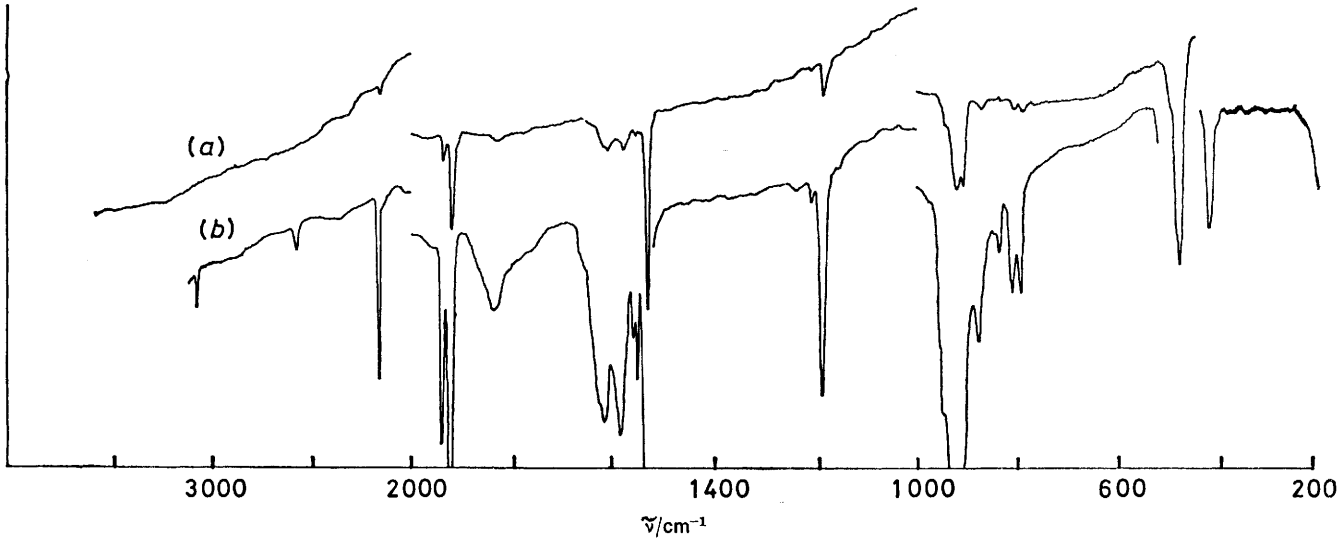

FIGURE 6 Infrared spectrum of solid $Zr(BD_4)_4$. Detail as in Figure 5

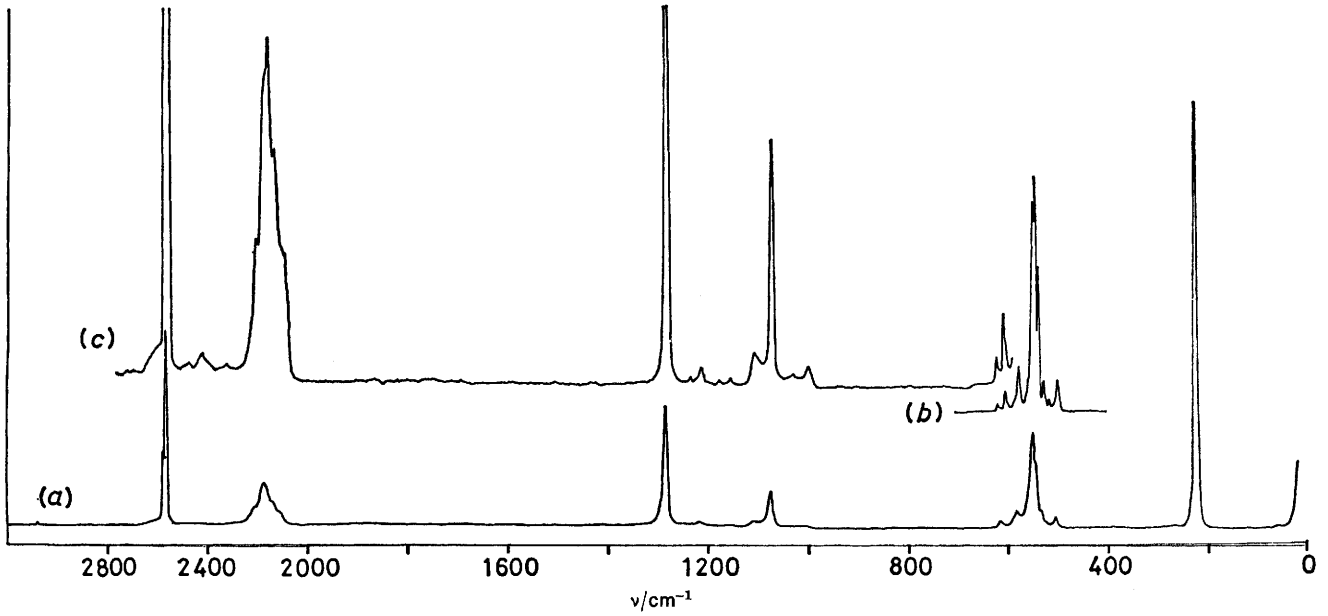

FIGURE 7 Raman spectrum of solid $Zr(BH_4)_4$ using a liquid-nitrogen cryostat. Spectra (*a*)—(*c*) were recorded under slightly different experimental conditions and are presented at different vertical amplifications

* Investigation of one batch of $Li[BD_4]$ by ^1H n.m.r. spectroscopy revealed an H content of between 1.0 and 1.5%.

13.8 and 23.6% of the molecules will contain a single ^1H nucleus and between 1.0 and 3.6% will contain two ^1H nuclei. The molecules $ZrB_4D_{15}H$ and $ZrB_4D_{14}H_2$ are of clearly distinguished from the modes of ZrB_4D_{16} in Figures 2, 4, 6, and 8 in that they occur in regions comparable with $Zr(BH_4)_4$ fundamental frequencies and

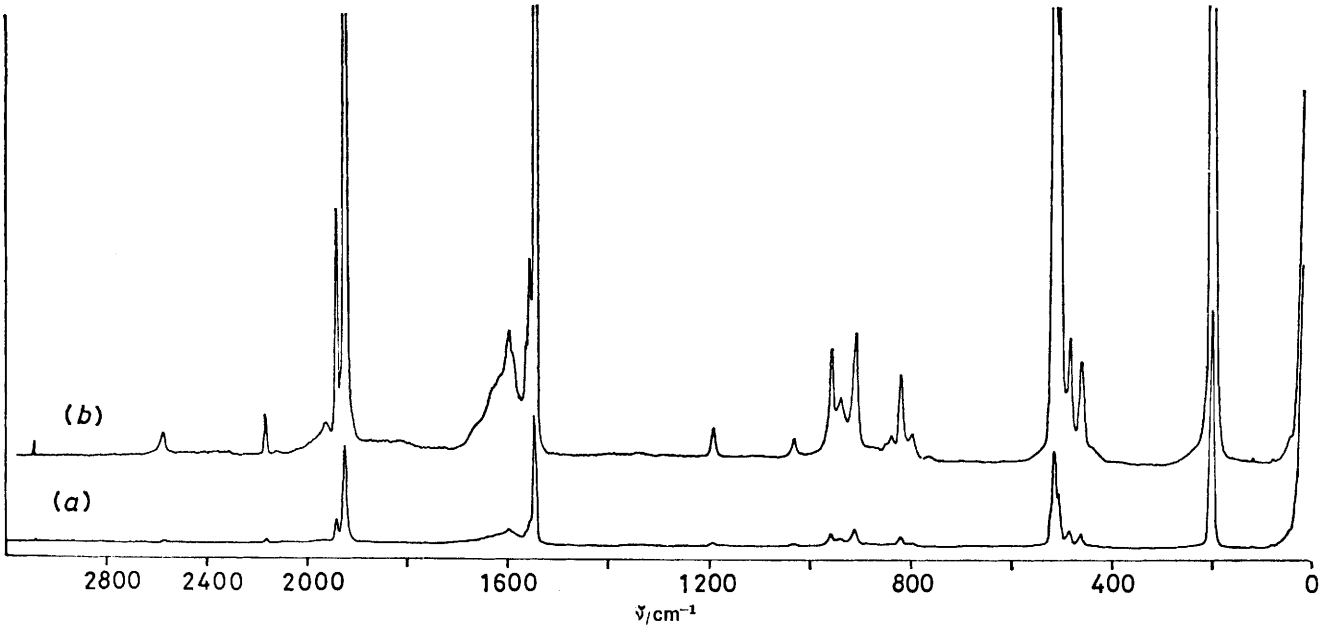

FIGURE 8 Raman spectrum of solid $Zr(BD_4)_4$, using a liquid-nitrogen cryostat. Spectrum (*b*) is a vertical amplification of (*a*)

relatively low symmetry (C_3, C_2, or containing only the identity symmetry element) and numerous i.r. and Raman fundamentals are predicted. First, modes predominantly due to ^1H motion are expected. These are

TABLE 3

Wavenumbers (cm^{-1}) of some overtone and combination bands in the spectra of $Zr(BH_4)_4$ and $Zr(BD_4)_4$

Solution		Solid		Assignment *
I.r.	Raman	I.r.	Raman	
(*a*) $Zr(BH_4)_4$				
		2 605vw	2 600vw (sh)	$\nu_{14} + \nu_{23}$
		2 524w		
2 481w		2 494w		$\nu_{15} + \nu_{16}$
2 419w		2 434vw		$2\nu_{16}$
	2 414vw		2 425vw	$\nu_6 + \nu_{10}$ ($2A + E$)
		1 871vw		$\nu_{15} + \nu_{21}$
1 785vw		1 797vw		$\nu_{16} + \nu_{21}$
			1 235vvw	
			1 155vvw	
		1 125vw		$\nu_{21} + \nu_{22}$
		1 041 (sh)	1 033vvw	$\nu_{22} + \nu_{23}$
		998vw	1 000vw	$2\nu_{23}$
(*b*) $Zr(BD_4)_4$				
		3 133vvw		$\nu_{13} + \nu_{14}$ or $\nu_{12} + \nu_{14}$
		3 058vw		$2\nu_{14}$
		1 958vw		$\nu_2 + \nu_{21}$ (F) or H species
1 862w		1 835w,br		$2\nu_{16}$ or $\nu_{15} + \nu_{16}$
	1 818vvw			
1 303vw				$\nu_{16} + \nu_{23}$
		946 (sh)		$2\nu_{23}$ or H species

* Except where noted, all the overtones and combinations have symmetry species $A + E + 2F$ of the T point group.

are polarized in the Raman solution spectrum. In addition, bands arising predominantly from deuterium

TABLE 4

Correlations of the vibrations of a triply bridged ZrH_3BH_t moiety of C_{3v} point group with those of $Zr(BH_4)_4$ molecules of T_d and T symmetry

$ZrBH_4$ Group C_{3v}	$Zr(BH_4)_4$ Molecule T_d	T	Approximate description of vibrational mode *	Observed wavenumber region (cm^{-1})
A_1	$A_1 + F_2$	$A + F$	B–H_t str.	2 560—2 580
A_1	$A_1 + F_2$	$A + F$		
E	$E + F_2 + F_1$	$E + 2F$	B–H_b str.	2 100—2 250
A_1	$A_1 + F_2$	$A + F$		
E	$E + F_2 + F_1$	$E + 2F$	HBH bend + ZrH_b str.	1 000—1 300
E	$E + F_2 + F_1$	$E + 2F$		
E	$E + F_2 + F_1$	$E + 2F$	Zr–H_b str. (' bridge def.')	500—650
A_1	$A_1 + F_2$	$A + F$	Zr–BH_4 str.	500—560
	$A_2 + F_1$	$A + F$	Zr–BH_4 torsion	250—650?
	$E + F_2$	$E + F$	BH_4–Zr–BH_4 bend	200—230

* The descriptions provided derive from force-constant calculations.

motion are observed in the vicinity of $Zr(BD_4)_4$ fundamentals. While numerous such modes are predicted, considerable accidental degeneracy is expected. Further, while many of these will formally be totally symmetric, their observed depolarization ratios may not differ greatly from that expected for non-totally symmetric vibrations. Thus, in the spectra of $Zr(BD_4)_4$ it is

difficult to separate unambiguously the latter modes of $ZrB_4D_{15}H$ and $ZrB_4D_{14}H_2$ from those of $Zr(BD_4)_4$.

Predictions based on symmetry. In the following paragraphs, assignments for $Zr(BH_4)_4$ and $Zr(BD_4)_4$ are discussed on the basis of the T and T_d symmetry point groups. Frequencies quoted, unless otherwise stated, pertain to the Nujol solution spectra for which Raman polarization data are available.

The high symmetry of the molecule gives rise to many degenerate normal modes, so that the 57 vibrational degrees of freedom form only 24 different normal modes. These can be divided into the symmetry species of the T and T_d point groups in (1) and (2) respectively. At

$$\Gamma_{vib} = 5A(\text{Raman}) + 5E(\text{Raman}) + 14F(\text{i.r., Raman}) \quad (1)$$

$$\Gamma_{vib} = 4A_1(\text{Raman}) + A_2(\text{inactive}) + 5E(\text{Raman}) + 5F_1(\text{inactive}) + 9F_2(\text{i.r., Raman}) \quad (2)$$

first sight it appears that a decision on the molecular symmetry (T or T_d) should be possible on the basis of the number of observed i.r. and Raman bands. Thus, T symmetry requires 14 i.r. and 24 Raman bands (14 of the latter being coincident with i.r. features). On the other hand, T_d symmetry predicts nine i.r. and 18 Raman bands with nine coincidences. The lower symmetry of the T structure makes the inactive A_2 and $5F_1$ modes of the T_d structure become allowed. However, it is a relatively small structural change, so that the new A and F modes are not expected to be strong. Furthermore, the A_2 and one of the F_1 modes of the T_d structure are torsional modes and in most known cases where torsional modes are allowed in the spectra they give rise to only very weak broad bands.

Full assignments based on the two symmetries are given in Tables 1 and 2, with species of the T_d point group given in parentheses.

B–H *Terminal stretching modes.* The B–H_t stretching region can provide no evidence for the structure (T or T_d) of $Zr(BH_4)_4$, since both models predict one totally symmetric Raman-active and one triply degenerate i.r.- and Raman-active mode. The two B–H_t stretching vibrations are readily assigned to the strong i.r. band at 2 567 cm^{-1}, $F(F_2)$ species, and the strong polarized Raman line, $A(A_1)$ symmetry, at 2 566 cm^{-1}. $Zr(BD_4)_4$ counterparts are observed at 1 920 (i.r.) and 1 919 cm^{-1} (Raman, p). In the spectra of $Zr(BD_4)_4$, bands at 2 565 (i.r.) and 2 567 cm^{-1} (Raman) are undoubtedly due to the B–H_t stretching mode of $ZrB_4D_{15}H$ (with the H nucleus in a terminal position). Shoulders at 1 934 (Raman, probably polarized) and 1 935 cm^{-1} (i.r.) are assigned to terminal B–D stretching modes of $ZrB_4D_{15}H$.

B–H *Bridge stretching modes.* A single ZrH_3BH_t group (point group C_{3v}) would have one A_1 and one E vibration involving stretching of the three B–H_b bonds. When four BH_4 groups are attached to the central Zr atom the B–H_b stretching modes give rise to $A + E + 3F$ ($A_1 + E + F_1 + 2F_2$) modes. The spectral predictions are: for T symmetry, five Raman + three i.r.; and for T_d symmetry, four Raman + two i.r., with one polarized Raman line in each case.

The strongest feature in the B–H_b(bridge) stretching region of the Raman spectrum of $Zr(BH_4)_4$ appears at 2 176 cm^{-1}, is polarized, and hence is due to the $A(A_1)$ symmetry mode. Two strong i.r. bands at 2 180 and 2 115 cm^{-1} are assigned to $F(F_2)$ modes. The $E(E)$ mode expected in this region (Table 4) is identified as the Raman shoulder at 2 207 cm^{-1} which shows no i.r. coincidence. There appear to be two possibilities for the remaining $F(F_1)$ mode. While no further bands are apparent in the i.r. solution spectrum, a shoulder at 2 199 cm^{-1} is discernible in the solid-phase i.r. spectrum (Figure 5). In addition, it is likely that the poorly distinguished Raman intensity in the 2 100—2 145 cm^{-1} region of both solution and solid-phase spectra is due to more than just the Raman counterpart of the strong i.r. F mode observed at 2 115 (solution) and 2 107 cm^{-1} (solid). If either of these possibilities is due to an F species fundamental of $Zr(BH_4)_4$ then this would support the T symmetry model.

In the spectra of $Zr(BD_4)_4$, the bands at 2 161 (i.r.) and 2 162 cm^{-1} (Raman, p) are certainly due to B–H_b stretching in $ZrB_4D_{15}H_b$. The B–D stretching region of both i.r. and Raman spectra, however, is rather complicated. The strong i.r. band at 1 539 cm^{-1} and strong Raman band at 1 547p cm^{-1} are readily assigned to $F(F_2)$ and $A(A_1)$ fundamentals, respectively, of $Zr(BD_4)_4$. The Raman line at 1 606 cm^{-1} is polarized (Figure 4) and must be assigned to a totally symmetric mode. Since the only totally symmetric mode of $Zr(BD_4)_4$ expected in this region (Table 3) has already been assigned, the weaker feature at 1 606 cm^{-1} is most probably due to symmetric B–D_b stretching in $ZrB_4D_{15}H$. In contrast, the lines at 1 591 and 1 625 cm^{-1} show a fairly high depolarization ratio and are coincident with well defined i.r. bands (1 589 and 1 626 cm^{-1}). These, then, are assigned to the remaining two $F(F_1 + F_2)$ fundamentals of $Zr(BD_4)_4$ expected in this region. This assignment, although not certain, is considered preferable to that previously suggested [3] for analogous vapour-phase i.r. features. The remaining weak i.r. and Raman features are assigned to proton-containing $Zr(BD_4)_4$ species, and it is not possible to choose an obvious counterpart for the E mode of $Zr(BH_4)_4$ at 2 207 cm^{-1}.

The region below 1 300 cm^{-1}. Having assigned seven normal modes of $Zr(BH_4)_4$ to B–H_t and B–H_b stretching there remain 17 fundamentals to be located. These all occur below 1 300 cm^{-1} and comprise $3A(2A_1 + A_2) + 4E(4E) + 10F(4F_1 + 6F_2)$ modes. As stated previously, one $A(A_2)$ mode and one $F(F_1)$ mode will involve BH_4 torsions and are expected to be weak. On the basis of mass, geometry, force constants, and vibrational spectra of tetrahydroborates, it is expected that vibrations involving H_bBH_t bending will occur in the 1 000—1 300 cm^{-1} region. Each H_3BH_t group contributes 3 H_bBH_t bends ($A_1 + 2E$ under C_{3v} symmetry).

These combine to give $A(A_1) + 2E(2E) + 5F(2F_1 + 3F_2)$ modes for $Zr(BH_4)_4$. There will, of course, be contributions from Zr–H_b stretching and H_bZrH_b bending to these vibrations, but it is not unreasonable to assign spectral features in this region to H_bBH_t stretching modes. The corresponding region for $Zr(BD_4)_4$ is 750—1 000 cm^{-1}.

In the low-wavenumber region the remaining seven fundamentals are expected. These are the skeletal stretching and deformation modes: $A(A_1) + 2E(2E) + 4F(F_1 + 3F_2)$. Suggested descriptions of these modes are given in Table 4.

H_bBH_t *Bending modes.* The strong polarized Raman band at 1 283 cm^{-1} is clearly due to an $A(A_1)$ mode. However, this band is believed to contain in addition E and $F(F_2)$ modes. The reasons for this are the relatively high depolarization ratio (Figure 3), the observation of an i.r. band $F(F_2)$ at 1 286 cm^{-1} which shifts to 937 cm^{-1} in the spectrum of $Zr(BD_4)_4$, and the splitting of the Raman band at 1 283 cm^{-1} into two components, 945(p) and 907(dp) cm^{-1}, in the spectrum of $Zr(BD_4)_4$. The line at 907 cm^{-1} shows no i.r. coincidence and is therefore assigned to an E mode. A depolarized Raman line at 1 075 cm^{-1} shifts to 814 cm^{-1} in the spectrum of $Zr(BD_4)_4$. Neither band has a coincidence in the i.r. and the assignment to an E species vibration is straightforward.

In addition to the i.r. band at 1 286 cm^{-1} discussed above, four other absorptions are observed at 1 213s, 1 170 (sh), 1 098w, and 1 056w cm^{-1}. These may be F modes (if the molecular symmetry is T), or any two of them may be F_2 modes of the T_d model. The shoulder at 1 170 cm^{-1} on the strong band at 1 213 cm^{-1} appears as a more clearly resolved peak in the vapour-phase [3] and solid (Figure 5) spectra. There is, however, no obvious Raman coincidence. The weak band at 1 098 cm^{-1} in the solution-phase i.r. spectrum may correspond to a shoulder at 1 085 cm^{-1} in the solid, or to a weak line in the Raman spectrum of the solid at 1 108 cm^{-1}. Finally, the weak feature at 1 056 cm^{-1} is observed at 1 058 cm^{-1} in the solid, but has no Raman counterpart.

The two bands at 1 286 and 1 213 cm^{-1} can be correlated with the i.r. bands of $Zr(BD_4)_4$ at 937 and 911 cm^{-1}. At present, however, it is not possible to assign unambiguously the three lower-frequency $F(2F_1 + F_2)$ modes expected in the i.r. spectra of $Zr(BD_4)_4$. Weak bands are observed at 830 and 809 (solution), 812 (vapour), and 877, 837, 811, and 793 cm^{-1} (solid). The choice is difficult, but a plausible assignment is given in Table 2. Infrared features at 1 185 and 1 026 cm^{-1} and the polarized Raman line in the spectra of $Zr(BD_4)_4$ at 1 186 cm^{-1} are assigned to $ZrB_4D_{15}H$.

Skeletal modes. There are two groups of low-frequency bands observed near 550 and 220 cm^{-1}. These are certainly due to vibrations involving skeletal motions such as Zr–BH_4 stretching, Zr–H_b stretching, and H_b–Zr–H_b bending. A combination of the latter two could also be described as ' bridge deformation '. BH_4 torsions are also expected to be observed at low frequencies. Since many of these modes involve motion of the boron atom, a complication of the spectra may arise from ^{10}B species. This is then a most difficult region to assign. A strong polarized Raman band at 544 cm^{-1} in the spectrum of $Zr(BH_4)_4$ shows only a small shift to 504 cm^{-1} for $Zr(BD_4)_4$ and is therefore assigned to the totally symmetric skeletal Zr–BH_4 stretch $A(A_1)$.

In the i.r. spectra of all samples of $Zr(BH_4)_4$ (vapour, solution, and solid) a single band at 504—507 cm^{-1} dominates. This band has a broad high-frequency shoulder at *ca.* 575 cm^{-1} in the vapour and solution spectra which becomes resolved into two bands at 547 and 581 cm^{-1} in the spectrum of the solid. This intensity pattern is replaced in the i.r. spectrum of all the samples of $Zr(BD_4)_4$ by a strong band at 483—484 cm^{-1} and a band of medium intensity at 418—425 cm^{-1}. The strongest of the i.r. bands for $Zr(BH_4)_4$ (504 cm^{-1}) and $Zr(BD_4)_4$ (484 cm^{-1}) are assigned to an $F(F_2)$ skeletal stretching mode, ν_{23}. This assignment is in keeping with the low ν_H/ν_D value expected for such a vibration and is consistent with the results of force-constant calculations (see later). Raman analogues are observed at 504 and 487 cm^{-1}.

The solid-phase i.r. bands at 581 and 547 are assigned to the bridge-deformation modes ν_{21} and ν_{22} of species $F(F_2$ and $F_1)$. Calculations indicate that the corresponding frequencies in $Zr(BD_4)_4$ should occur near 400 cm^{-1} (Table 6). However, only one band is observed in this region of the spectra of the heavy molecule and this is assigned to $\nu_{21}[F(F_2)]$.

TABLE 5

Modified valence force field for $Zr(BH_4)_4$

Internal co-ordinates	Value [a]
(*a*) Valence force constants	
B–H_t str.	3.60
B–H_b str.	2.55
Zr–H_b str.	0.40
H_tBH_b bend	0.41
H_bBH_b bend	0.44
B–Zr–B bend	0.84
Zr–B str.	1.50
(*b*) Interaction force constants	
B–H_t–B–H_b	0.06
B–H_b–B–H_b	0.03
H_tBH_b–H_tBH_b	0.03
H_tBH_b–H_bBH_b [b]	0.005
H_tBH_b–H_bBH_b [c]	0.035
H_bBH_b–H_bBH_b	0.03
Zr–B–Zr–B	0.15

[a] Units are mdyn $Å^{-1}$ for stretching, mdyn Å for bending, and mdyn for stretch–bend interaction force constants. [b] Angles H_tBH_b and H_bBH_b do not have a B–H_b bond in common. [c] Angles H_tBH_b and H_bBH_b have a B–H_b bond in common.

In the solution and solid-phase i.r. spectra of $Zr(BD_4)_4$ shoulders are observed at 511 and 506 cm^{-1}, respectively. These are most likely due to the Zr–B stretching modes of $ZrB_4D_{15}H$. Thus, the partially resolved multiplet between 518 and 502 cm^{-1} in the

Raman spectrum of $Zr(BD_4)_4$ is considered to contain components due to the symmetric skeletal stretching modes of both ZrB_4D_{16} [with $Zr(BH_4)_4$ analogues at 549—557 cm^{-1}] and $ZrB_4D_{15}H$.

While the assignment of the skeletal stretching modes appears reasonably clear, there is little to suggest which of the remaining bands are due to torsional modes (forbidden under T_d symmetry) and which are due to and/or 610 cm^{-1}) is uncertain, possibly arising from torsional and/or bridge-deformation modes.

Overtones and combinations. A number of very weak features in the spectra of both $Zr(BH_4)_4$ and $Zr(BD_4)_4$ could not be attributed to fundamentals. These are listed in Table 3 with possible assignments in most cases.

Application of the isotope product rule. The Redlich–Teller isotope product rule, as formulated in Herzberg's

TABLE 6

Calculated and observed wavenumbers (cm^{-1}) for $Zr(BH_4)_4$ and $Zr(BD_4)_4$ and the calculated potential distribution (p.e.d.) for $Zr(BH_4)_4$

Symmetry		$Zr(BH_4)_4$		$Zr(BD_4)_4$		P.e.d.[b] (%) for $Zr(BH_4)_4$							Suggested nomenclature for normal modes
T	T_d	Obs.	Calc.[a]	Calc.[a]	Obs.	$B–H_t$	$B–H_b$	$Zr–H_b$	H_tBH_b	H_bBH_b	BZrB	Zr–B	
A	(A_1) ν_1	2 567	2 582	1 927	1 922	99							$B–H_t$ str.
	(A_1) ν_2	2 165	2 139	1 531	1 544		96	1					$B–H_b$ str.
	(A_1) ν_3	1 285	1 296	957	954			35	30	35		1	HBH bend
	(A_1) ν_4	543	549	492	504		1	18	1	2		60	Zr–BH_4 str.
	(A_2) ν_5	*ca.* 275?			*ca.* 201?								Zr–BH_4 torsion
E	(E) ν_6	2 210	2 198	1 651		99	1	1					$B–H_b$ str.
	ν_7	1 283	1 234	874	908		1	27	61	23			HBH bend
	ν_8	1 075	1 057	797	817		1		23	76	1		HBH bend
	ν_9	533	558	403	*ca.* 435?			71	22	9	1		$Zr–H_b$ str. bridge def.
	ν_{10}	224	224	193	198			1	1		98		BH_4–Zr–BH_4 bend
F	(F_2) ν_{11}	2 571	2 580	1 922	1 920	99							$B–H_t$ str.
	(F_1) ν_{12}	2 199	2 197	1 649	1 616		99	1	1				$B–H_b$ str.
	(F_2) ν_{13}	2 180	2 196	1 646	1 585		99	1	1				$B–H_b$ str.
	(F_2) ν_{14}	2 115	2 139	1 530	1 536		96	1					$B–H_b$ str.
	(F_2) ν_{15}	1 286	1 295	952	924			36	30	35		1	HBH bend
	(F_2) ν_{16}	1 217	1 235	876	909		1	27	61	23			HBH bend
	(F_2) ν_{17}	1 178	1 234	874	837		1	27	61	23			HBH bend
	(F_1) ν_{18}	1 098	1 056	794	811		1		24	76			HBH bend
	(F_1) ν_{19}	1 058	1 052	788	793		1		24	76			HBH bend
	(F_1) ν_{20}	610?			458?								Zr–BH_4 torsion
	(F_2) ν_{21}	581	572	405	418			62	19	8	2	13	$Zr–H_b$ str., bridge def.
	(F_1) ν_{22}	547	555	398				72	23	8			$Zr–H_b$ str., bridge def.
	(F_2) ν_{23}	504	521	498	483		1	30	6	4		66	Zr–BH_4 str.
	(F_2) ν_{24}	216	210	185				1	1		97	1	BH_4–Zr–BH_4 bend

[a] Torsions were not included in the normal co-ordinate analysis. [b] All the values are rounded off to the nearest integer, and derive from a p.e.d. calculated for all the force constants in Table 5. Only the valence force constants are given above, however, and for this reason the sum of p.e.d. contributions for any particular mode is not equal to 100% in the Table.

bridge-deformation modes. The assignments given in Tables 1 and 2 are tentative.

Skeletal bending modes are identified as low frequencies which show relatively small ν_H/ν_D values. The E and F symmetry modes are resolved in the solid phase $Zr(BH_4)_4$ spectra, with the E mode at 224 cm^{-1} (Raman effect only) and the F mode at 216 cm^{-1} (i.r., Raman coincidence).

The assignments and observations from the present work, pertaining to the region below 700 cm^{-1}, can be compared with those of Tomkinson and Waddington [19] derived from inelastic neutron scattering (i.n.s.) data. We believe that their assignment to bridge-deformation modes of a wavenumber of 116 cm^{-1} is in error, since no Raman line was observed near this region. This being the case, the assignment of the i.n.s. frequency at 594 cm^{-1} (probably equivalent to the Raman bands at 581

book,[20] can be used to predict ratios of products of wavenumbers, within each symmetry species, for normal and fully deuteriated $Zr(BH_4)_4$. For these calculations, the moments of inertia obtained from the electron-diffraction structural data [4] are 379.36×10^{-40} g cm^2 for $Zr(BH_4)_4$ and 498.90×10^{-40} g cm^2 for $Zr(BD_4)_4$. The total molecular masses are 151.38 and 167.48, respectively. These values are for the ^{11}B isotopic species in each case.

For the five E modes of both T and T_d models the calculated ratio is 0.250. From Table 6 we have five assigned wavenumbers for $Zr(BH_4)_4$ but for $Zr(BD_4)_4$ only ν_7, ν_8, and ν_{10} have been located. Using these three together with calculated values for ν_6 and ν_9, we find an

[20] G. Herzberg, 'Infrared and Raman Spectra of Polyatomic Molecules,' Van Nostrand, Princeton, New Jersey, 1945, p. 232.

' observed ' product ratio of 0.272 which is reasonably close to the theoretical value.

For the totally symmetric modes the predictions are 0.250 for five A species of the T point group or 0.354 for four A_1 species of T_d. For the latter case, taking observed values for ν_1—ν_4 gives an observed ratio of 0.367. For the T point group, wavenumber values are needed for the symmetric torsion in each molecule. A band at 275 cm^{-1} was tentatively assigned to this mode in $Zr(BH_4)_4$ and there is a shoulder at 201 cm^{-1} in the Raman spectrum of $Zr(BD_4)_4$. Using these wavenumbers for ν_4 leads to an experimental isotope product ratio of 0.272.

For the nine F_2 species fundamentals of the T_d model the theoretical isotope product ratio is 0.106 4. Taking the corresponding observed wavenumbers from Table 6, the calculated ratio is 0.102 7. On the other hand, for the 14 F species modes of the T point group the theoretical ratio is 0.027 4 including the torsions. The ratio of the observed wavenumber products is 0.021 9.

Lattice modes. The space group reported for solid $Zr(BH_4)_4$ was $P\bar{4}3m$ (T_d^1) with one molecule per unit cell.[1] This implies that unit-cell, site, and molecular point groups must all be T_d. There is only one triply degenerate rotatory lattice mode of species F_1, which is inactive in both Raman and i.r. However, the X-ray diffraction study did not locate the bridging hydrogen atoms reliably and if the reported gas-phase molecular structure (T) is carried over into the solid state a slightly lower crystal symmetry would result. The results of the X-ray diffraction study might also fit space groups 195, 196, or 197, all of which have T unit cell and site symmetries and can have one molecule per unit cell. In this case the rotatory lattice mode is allowed in both i.r. and Raman spectra.

The experimental results seem to support the latter structure. There is quite clearly a shoulder at 45 cm^{-1} on the Raleigh line in the Raman spectrum of solid $Zr(BD_4)_4$ (Figure 8). A very weak band is also observed at 55 cm^{-1} in the spectrum of solid $Zr(BH_4)_4$. The expected isotope shift of the rotatory lattice mode should give a wavenumber ratio of 0.87 (from the square root of the ratio of the moments of inertia). The shift of the observed lattice mode gives a ratio close to this value.

Normal Co-ordinate Analysis.—The Wilson FG matrix method [21] was used for the calculations, which were performed on a PDP 10 computer at the University of Queensland and on IBM 360-50 and Burroughs 6700 computers at Queen's University, Kingston, Ontario. Computer programs were based on those originally written by Schachtschneider [22] and modified by Brooks [23] and ourselves.

Initial calculations were made on both T_d and T molecular models of $Zr(BH_4)_4$. Bond lengths and angles were taken from electron-diffraction results.[4] The value of the torsion-dependent angle H_b–B–Zr–B was taken as 40° for the T model, which is close to the electron-diffraction value of 38°. For the T_d model this angle ϕ is either 0 or 60° (see Figure 1 of ref. 5).

The actual computational differences between the T and T_d models are small. The same set of internal co-ordinates can be used for both models, which through the different choices of ϕ (40° for T and 60° for T_d) give slightly different G matrices. Using the same simple valence force field (diagonal elements only) identical sets of frequencies were obtained for both models. Only the introduction of certain interaction constants can lead to small differences in frequencies and potential-energy distributions.

It was decided to proceed with a calculation based on T symmetry, since a fairly complete set of observed wavenumbers together with electron-diffraction structural data was available for this model. Refinement of the force field was carried out until a reasonable overall fit between observed and calculated wavenumbers was obtained for $Zr(BH_4)_4$. Then, finally, a set of wavenumbers was calculated for $Zr(BD_4)_4$. A set of internal co-ordinates was chosen so as to form the smallest set likely to yield the most physically meaningful force field. These included 4 × B–H_t, 12 × B–H_b, 12 × Zr–H_b, and 4 × Zr–B bonds as well as 12 × H_tBH_b, 12 × H_bBH_b, and 6 × BZrB angles. Internal co-ordinates corresponding to torsions of the BH groups around Zr–B bonds were excluded. Thus, 62 internal co-ordinates are used to describe 53 vibrational degrees of freedom. Sixty-two symmetry co-ordinates were devised in the usual manner.[21,24] These resulted in the calculation of the correct number and symmetry distribution of zero frequencies corresponding to the nine inherent redundancies. As a check on the symmetry factoring of the secular equation, calculations based on unsymmetrized F and G matrices were performed. These gave the same results as those based on the symmetrized F and G matrices.

A simple valence force field yielded a reasonable observed–calculated frequency fit, with perhaps the major improvement deriving from the introduction of the Zr–B–Zr–B interaction constant. While other interaction constants (Table 5) yielded further improvements in the numerical fit, little weight can be placed on the significance of the values of these additional constants. Although, no doubt, further improvement could have been gained by the inclusion of still further interaction constants (particularly inter-BH_4 rather than intra-BH_4 group interactions), there seemed little point to such an exercise, given the limitations of the methodology for a molecule so large. Nevertheless, the frequency fit shown in Table 6 and the force field in Table 5 are considered sufficient to determine

[21] E. B. Wilson, J. C. Decius, and P. C. Cross, ' Molecular Vibrations,' McGraw-Hill, New York, 1955.
[22] J. H. Schachtschneider, Technical Report no. 57–65, Shell Development Co., 1965.
[23] W. V. F. Brooks, personal communication.
[24] F. A. Cotton, ' Chemical Applications of Group Theory,' Wiley–Interscience, New York, 1971.

the dominant characteristics of the vibrations of $Zr(BH_4)_4$.

Although the modified valence force field derived in the present work cannot be compared precisely with the force fields obtained for diborane and the $[BH_4]^-$ ion (see for example refs. 25 and 26), the current force-constant values do seem physically reasonable. The $B-H_t$ stretching constant (3.6 mdyn Å^{-1}) * is greater than the B–H stretching constant for the $[BH_4]^-$ ion (evaluated as *ca.* 2.8 mdyn Å^{-1} by most studies) which in turn is greater than the $B-H_b$ stretching constant (2.55 mdyn Å^{-1}). The ratio of $B-H_b$ to $B-H_t$ stretching constants (0.71) is greater than the corresponding ratio for diborane (*ca.* 0.5). Angle-bending force constants for H_t-B-H_b and H_b-B-H_b (0.41 and 0.44 mdyn Å^{-1}, respectively) are within the range of values obtained for analogous constants in diborane. The value of the $Zr-H_b$ stretching force constant (0.4 mdyn Å^{-1}) is conspicuously low. A terminal Zr–H stretching frequency of 1 620 cm^{-1} has been observed [2] for the compound $Zr(BH_4)(C_5H_5)_2H$. A number of compounds containing Zr–H–Zr bridges [27] show bands in the range 1 240—1 520 cm^{-1}. A comparison of these data with the results of the present work yields the reasonable order of Zr–H stretching force constants: $Zr-H_t > Zr-H_b-Zr > Zr-H_b-B$. This low value of f(Zr–H) is also quantitatively consistent with the low $Zr-H_b$ bond order (0.18) deduced [4] from bond-length considerations, a value which approximates that (0.13) estimated [8] for Hf–H in $Hf(BH_4)_4$ from polarizability calculations. The inclusion of an explicit Zr–B stretching force constant in the present calculations [f(Zr–B) 1.5 mdyn Å^{-1}] is consistent with the conclusion arising from other sources [8,28] that M–B bonding (M = Zr or Hf) may be significant in the compounds $M(BH_4)_4$.

A separate set of calculations was performed employing a symmetry force field and a set of internal co-ordinates identical to those above except for the exclusion of the Zr–B co-ordinate. This was sufficient to account for all the vibrational degrees of freedom of $Zr(BH_4)_4$ (except for the $A + F$ torsions) and readily yielded good fits for all the frequencies except those assigned to Zr–B ($A + F$) skeletal stretches. This result is consistent with, but not proof of, the existence of some direct metal–boron bonding.

The force field reported here is broadly consistent with a view that the covalency of the bonding of the BH_4 group in $Zr(BH_4)_4$ is intermediate between that in diborane and that in the alkali-metal tetrahydroborates. Force-constant calculations have been reported previously [8] for $Hf(BH_4)_4$. That the latter problem was formulated in terms of a somewhat different set of internal co-ordinates, utilized a different set of interaction constants, and apparently assumed a different H–D correlation for the triply degenerate skeletal-stretching mode than in the present work implies that the $Hf(BH_4)_4$ and $Zr(BH_4)_4$ force fields cannot be compared in fine detail. Within these limitations, however, it is apparent that the results obtained for the two molecules are compatible.

The potential-energy distribution (p.e.d.) calculated from the force field in Table 5 and given in Table 6 forms the basis for the suggested descriptions of the normal modes of $Zr(BH_4)_4$ presented in Table 6. Bands in the 2 560—2 580 cm^{-1} region are pure $B-H_t$ stretches, those between 2 100 and 2 250 cm^{-1} pure $B-H_b$ stretches and those between 210 and 230 cm^{-1} pure skeletal bands. A $B-H_b-B-H_b$ stretching interaction constant contributes slightly (>3% absolute) to the $B-H_b$ stretching modes. All the remaining frequencies, however, show significant contributions from more than one type of force constant. The modes ν_4 and ν_{23} are characterized by a major contribution from f(Zr–B) and a significant contribution from f(Zr–H). These are therefore described as $Zr-BH_4$ skeletal stretches. The Zr–B–Zr–B interaction constant contributes mainly to ν_4 (18%) and ν_{23} (−7%).

The p.e.d. for $Zr(BD_4)_4$ indicates that the calculated H ⟶ D correlation for ν_{23} is 521 ⟶ 498 cm^{-1}, consistent with the observed H ⟶ D shift (504 ⟶ 483 cm^{-1}) proposed earlier.[8] The potential energies of modes occurring between 1 000 and 1 300 cm^{-1} derive, predominantly, from HBH bending force constants, and the broad description of HBH bending is suggested. The various HBH bend–bend interaction constants contribute mainly to frequencies in the 1 000—1 300 cm^{-1} region and less so to the bridge-deformation modes. This contrasts with the formal description of 'Zr–H stretching' applied previously [3,12] to modes analogous to the higher-frequency vibrations in this region. While the detailed differentiation between the modes in the 1 000—1 300 cm^{-1} region shown in Table 5 is considered an oversimplification (as gauged from the observed–calculated frequency fit), it is noted that the higher-frequency vibrations do show a significant contribution from the Zr–H stretching constant. Vibrations ν_9, ν_{21}, and ν_{22} derive mainly from $Zr-H_b$ stretching, and 'Zr–H_b stretching' or 'bridge deformation' are suggested as alternative descriptions.

Conclusions.—The i.r. and Raman spectra of $Zr(BH_4)_4$ can be assigned in terms of a T point group. However, the evidence is not unequivocal and the T_d structure has been given equal consideration. Observed features have been assigned to the additional six Raman (five i.r.) bands predicted by the selection rules of the lower-symmetry structure. In every case a very weak band was assigned, but this is not unexpected, since the difference between the T and T_d structures is small. The observation of a rotatory lattice mode is also

* Throughout this paper: 1 dyn = 10^{-5} N.

[25] T. Ogawa and T. Miyazawa, *Spectrochim. Acta*, 1964, **20**, 557.

[26] A. R. Emery and R. C. Taylor, *J. Chem. Phys.*, 1958, **28**, 1029.

[27] P. C. Wailes and H. Weigold, *J. Organometallic Chem.*, 1970, **24**, 405.

[28] T. J. Marks and L. A. Shimp, *J. Amer. Chem. Soc.*, 1972, **94**, 1542.

evidence for the T point group. However, the possibility that many of these weak bands arise from lower-symmetry mixed boron isotopic molecules cannot be ruled out. The normal co-ordinate analysis reported has provided useful descriptions of the normal modes of $Zr(BH_4)_4$ and has aided in the correlations between observed wavenumbers in the normal and deuteriated molecules. The necessity of a specific Zr–B stretching force constant supports the conclusion that Zr–B bonding is important in the molecule.

We thank Professor S. J. Cyvin, University of Trondheim, for helpful suggestions concerning the construction of symmetry co-ordinates for $Zr(BH_4)_4$, and the Australian Research Grants Committee and the National Research Council of Canada for support.

[7/962 *Received*, 3*rd June*, 1977]